Effects of Winding Speed, Drawing and Heating on the Crystalline Structure of Nylon 6 Yarns

H. M. HEUVEL and R. HUISMAN, *AKZO Research Laboratories, Fibre Research Department, Arnhem, The Netherlands*

Synopsis

Nylon 6 yarns were wound at speeds varying from 700 to 5500 mpm. The effect of the winding speed on both α- and γ-type crystals in these undrawn yarns was studied. Also the effects of dry heat, tension, and heating in saturated steam were included in this investigation, since they provide useful information for drawing and heat-setting processes. The emphasis was put on the characterization of the crystalline part of the yarns. By applying recently developed techniques, relative amounts of the two crystalline components, as well as their orientation factors, could be determined. Concerning the undrawn, conditioned yarns, it was found that the amount of γ type increases with the winding speed. The γ crystals are much better oriented than the α crystals, and the crystal dimensions of the γ structure largely depend on the winding speed in contrast to those of the α crystals. Indications were found that γ crystals are mainly generated from orientation-induced nuclei at speeds higher than 2500 mpm and that α crystals grow slowly at relatively low temperatures after moisture pickup during conditioning. Drawing at high ratios causes a transition from γ to α, while the thermal stability of the γ crystals appears to be slightly below that of the α crystals, resulting in γ crystal to α crystal transitions at extremely high temperatures or under usual autoclaving conditions.

INTRODUCTION

In nylon 6, two different crystalline modifications can be found. In the best known structure, the monoclinic α modification, the molecules are in the extended flat zigzag configuration and the hydrogen bonds are between antiparallel chains.[1] For the γ modification, which is much less well understood, we use the model proposed by Arimoto.[2-5] This implies a monoclinic unit cell with a molecular arrangement in the basal plane which is similar to that of the α crystals. The main difference with respect to the α structure is that the hydrogen bonds are between parallel molecules, forcing the chains to twist slightly in order to realize these bonds. Consequently, the γ unit cell is about 2% less in height. The shift between the hydrogen-bonded sheets of 3/14 in the vertical direction of the α crystals is absent. In Figure 1, the basal planes and the heights of both crystal types are depicted. The open triangles indicate the nylon 6 chains, the angles pointing in the same direction representing parallel molecules, those pointing in opposite direction standing for antiparallel chains. Half the γ picture of Figure 1 is dashed since it is not a real part of the unit cell for lack of a shift of the 001 planes.

The occurrence of the pure γ-phase crystals has only been reported for nylon 6 samples after an iodine treatment. In most chemically untreated nylon 6 films and yarns described in the literature, the α form predominates. By high-speed spinning and spin-draw-winding techniques, however, yarns are obtained which can contain mixtures of both crystal modifications. Our investigation was mainly concerned with the effect of the winding speed in the spinning process upon the

Journal of Applied Polymer Science, Vol. 26, 713–732 (1981)
 CCC 0021-8995/81/0026-0713$02.00

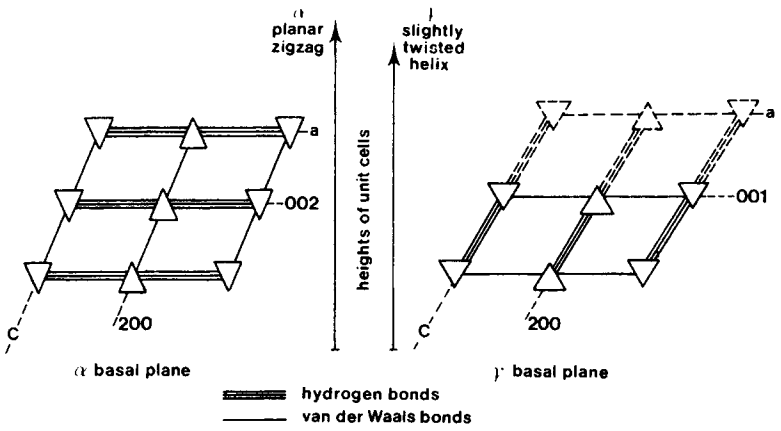

Fig. 1. Schematic presentation of the α- and γ-nylon 6 unit cells.

ratio between the amount of α- and γ-phase crystals and with a further detailed characterization of both. The next point of interest was the influence of temperature and tension during aftertreatments. Finally, the effect of autoclaving in saturated steam was studied since also this severe heat treatment is of great practical importance in heat-setting processes.

In order to carry out these investigations, quantitative x-ray information is needed. The problem is that in the diffraction pattern of nylon 6 no separate information about the α and γ phase is available. The only isolated γ diffraction peak, the 020 on the meridian, is not a reliable yardstick for the amount of this crystal modification.[6] For the α structure there is no isolated diffraction peak available at all. Most of the information is on the equator, but the various broad peaks are so poorly separated that the diffraction trace as such cannot be used for quantitative structural information. Therefore, a computer program was developed to resolve the equatorial diffraction pattern into five components related to both crystalline phases and the amorphous material.[7] A fitting procedure eventually provides information about the α and γ crystals, including molecular distances, crystal sizes, and radially integrated peak areas. This technique is not only applied to equatorial scans but also to radial scans made at various azimuthal angles and thus provides the possibility of obtaining crystalline orientation factors and relative amounts of both crystalline modifications.

CHARACTERIZATION OF THE α AND γ STRUCTURES

For the characterization of the two crystalline phases x-ray diffraction is the most suitable technique. In Figure 2(a) an Astbury picture of a nylon 6 yarn is presented. From this picture it is clear that the only isolated peak of considerable intensity is the one on the meridian. This meridional 020 peak is due to the γ-phase crystals but is not useful for the determination of the amount of γ crystals, because the intensity is extremely sensitive to small shifts of the molecules in the chain direction.[6] However, this diffraction peak can be used for the determination of the height of both the unit cell and the crystals of the γ phase. Also orientation measurements of the γ crystals can be carried out on

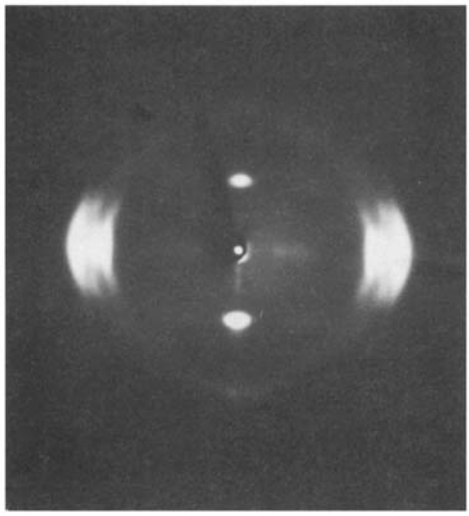

(a)

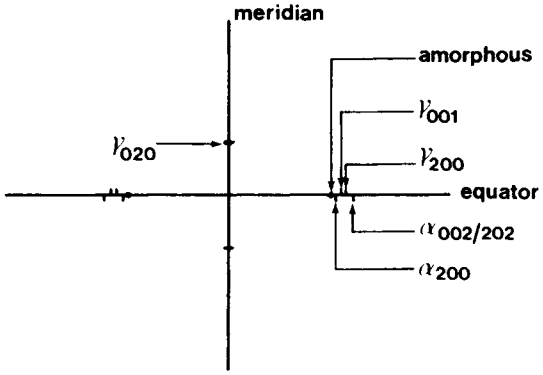

(b)

Fig. 2. (a) Astbury picture of a nylon 6 fiber containing both crystal modifications. (b) Schematic presentation of (a).

this isolated diffraction peak. For the α structure no isolated peak is available. On the equator there is much information, but the Astbury picture already shows the problem of a high degree of overlap between various peaks. In Figure 2(b), these various components are indicated schematically. To obtain information about each of these components, a diffractometer is used. In Figure 3(a), an example is shown of an equatorial diffractometer scan of a yarn containing a mixture of α and γ crystals. A computer program described in detail elsewhere[7] has been developed for the decomposition of such traces into two α peaks, two γ peaks, and an amorphous contribution. The results obtained are illustrated in Figure 3, which presents the calculated envelope in Figure 3(a) and the separate components in Figure 3(b).

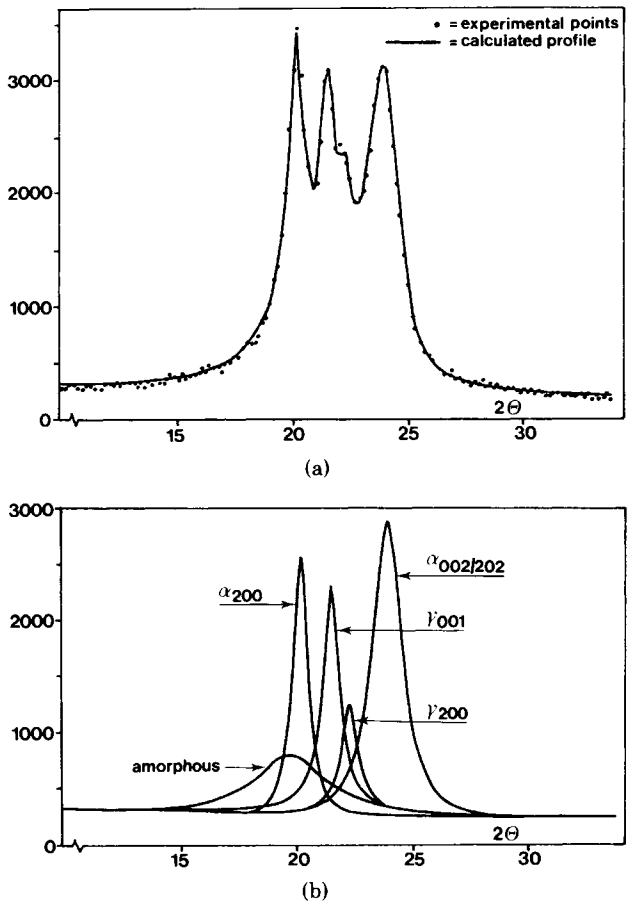

Fig. 3. (a) Fitting of the five-line model. (b) Composition of the envelope of (a).

From the peak positions, the molecular distances within the basal plane are calculated and from the half-widths the crystal thicknesses in the directions perpendicular to the planes involved. For simplicity, in the following only one crystal thickness parameter will be used for each crystal modification. As the effectiveness of crystal perfectioning is greatest in the direction in which the decrease of energy is most pronounced, the thickness along the hydrogen-bonded sheets is taken as the best characteristic. So, for the α crystals, the half-width of the 200 and for the γ crystals the 001 diffraction peak is used as the best crystal thickness parameter (Fig. 1). As such, diffraction intensities radially integrated over 2θ do not provide information on the amount of the two crystalline modifications. The intensity at the equator only originates from those crystals which are perfectly aligned along the fiber axis. Crystals with the molecular chains at some angle with respect to the fiber axis contribute to the off-equator intensity at some azimuthal angle. Therefore, the course of the radially integrated peak areas as a function of the azimuthal angle ϕ_e (see Fig. 4) is needed to obtain information on the amount of the two crystalline modifications. For this purpose, only one α and one γ peak has to be considered, as it has been shown[7] that both α peaks have the same orientation distribution in a yarn, just as both γ peaks

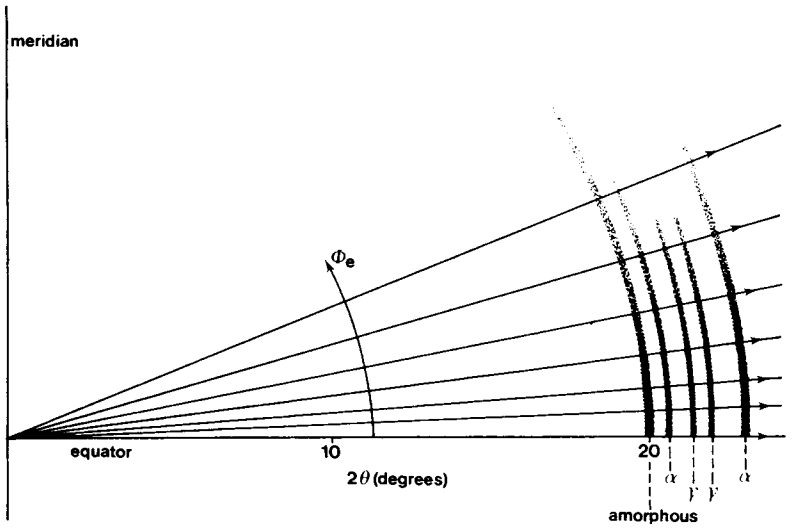

Fig. 4. Radial scans at various azimuthal angles.

have. From the course of these radially integrated peak areas with ϕ_e, not only the relative amounts but also the orientation factors of both crystal modifications can be calculated. Further details are described in ref. 7.

EXPERIMENTAL

Yarns

The experimental work can be divided into three parts with respect to the types of yarn investigated. The first part was concerned with as-spun filaments. The main objective was to study the relation between the winding speed and the amount of α and γ crystals, their physical properties and their origin. The spinning temperature was 290°C, and the chips used had a specific viscosity of 2.0 as measured in a 90% formic acid solution, 1 g polymer in 100 ml solute at 25°C. The diameter of the spinneret holes was 250 μm. The yarn bundles, consisting of ten filaments, were wound at speeds varying from 700 to 5500 mpm. The total yarn count varied from 268 dtex at 700 mpm to 99 dtex at 5500 mpm in order to get the same count after drawing.

The second part of the investigation was directed to the effect of dry heat and tension on the two crystalline phases. For this study the starting materials were undrawn yarns wound at speeds of 1460, 3630, and 5325 mpm. These yarns were heat treated at 150, 180, and 210°C, each temperature being combined with three levels of tension, viz., tensionless, low draw ratio, and high draw ratio. The indication "low draw ratio" is related to the situation with the lowest draw ratio at which a yarn could be made without undrawn parts. The high draw ratio is the highest ratio at which the process could be run without too many breaks.

In the third part, the effect of treatments with saturated steam was investigated. To this end, the as-spun fibers wound at 1460, 3630, and 5325 mpm were subjected to heat treatments in an autoclave at temperatures of 110, 120, and 130°C. The treatments were carried out tensionless.

Measuring Equipment

Differential Thermal Analysis. du Pont 990 TA with a cell base operating with a DSC cell at a heating rate of 20°C/min.

Birefringence. Zeiss polarizing microscope provided with Ehringhaus compensator at a wavelength of 589 nm with the filaments embedded in dichlorobenzene.

X-Ray Diffraction. The WAXS work was carried out with a Philips diffractometer provided with a quartz monochromator, Soller slits, a divergence slit (1°), a scatter slit (0.2 mm), and a receiving slit (1°). The diffractometer was directly coupled to a Hewlett–Packard counter, and every 5 sec the intensity was recorded automatically on magnetic tape. The transmission technique was used, and the range between 10° and 34° on and near the equator was scanned at the rate of 1°/min. The same speed was used for the meridional scanning between 7° and 15°.

Calculations. These were performed on a Harris slash 4 VMS and an IBM 3033 computer, using extended precision.

X-Ray Measurements and Application of the Computer Program

Normal equatorial x-ray measurements do not provide information on the relative amounts and orientations of the α- and γ-phase crystals. Like Garton et al.,[6,8] who carried out these measurements in a more qualitative way, we also performed measurements at various azimuthal angles ϕ_e around the equator (see Fig. 4). This procedure has already been described in an earlier paper in detail[7] but is summarized here again in order to make clear how we obtained our results. The range of ϕ_e values used was adapted experimentally to the course of the intensity with ϕ_e. So for the well-oriented yarns, the range used was from $-12°$ to $+12°$, and for the least-oriented sample, from $-30°$ to $+30°$. For each yarn, 13 radial scans were made at regular ϕ_e intervals, distributed symmetrically around the equator. The application of the five-line computer program already mentioned in the introduction is not possible for all ϕ_e values. The problem in the application of this model to scans made at ϕ_e values exceeding 5° is the possible interference of the γ 011,210 diffraction doublet on the first layer line at about $\phi_e = 15°$. To this end, special radial scans were made through the maximum of this spot for yarns which showed a substantial amount of well-developed γ crystals. By applying a six-line model, the peak position, half-width, and shape parameter of the line accounting for this γ 011,210 contribution could be established. This sixth line was included in all other calculations with only its intensity as a free parameter. Consequently, for each yarn, 13 scans had to be fitted with six lines with all parameters free except those mentioned in relation to the sixth line, the position and shape parameter of the amorphous contribution (values respectively 19.8° and 5) and the shape parameters of both γ-lines 001 and 200, fixed at the value of 1.4. As in this case the computer program contains 14 free parameters, no accurately determined parameter values can be expected from traces in which not all peaks are equally well developed. Therefore, for each yarn plots were made of all these 14 parameters, including their 2σ limits, versus ϕ_e. Parameters which did not change significantly with ϕ_e were fixed at an average value. It turned out that only the six intensities and the half-widths of the two α lines, 200 and 002/202, and sometimes those of the two γ lines, 001

and 200, could not be fixed. In a second cycle, all sets of 13 scans were fitted again, now with only these parameters free. The results turned out to be quite satisfactory, good fits being combined with a considerably improved parameter accuracy.

To obtain the relative amounts of α and γ, the radially integrated peak areas of the α 200 peak and those of the γ 001 peak have to be integrated over the azimuthal angle ϕ_e. In this way, the total "volume" of the reflection is calculated. As a result of the coupling between the areas of the two radially integrated α-peaks[7] and another coupling for the two γ-peaks, azimuthal integration over ϕ_e of the α 002/202 and the γ 200 does not provide any additional information. Before integration, the radially integrated peak intensities have to be multiplied by cos ϕ_e, as in diffractometer scanning a kind of ϕ_e-dependent dilution takes place which has to be corrected for.[9] To obtain the "relative γ-number," the double integrated γ intensity, i.e., in radial and azimuthal direction, is divided by the sum of both α and γ double-integrated intensities.

Also the orientation factors can be calculated for both crystal types, by making use of the course of the radially integrated peak areas with ϕ_e. To this end, the value $\langle \cos^2 \phi_e \rangle$ for both α and γ has to be calculated as

$$\langle \cos^2 \phi_e \rangle = \frac{\int_0^{\pi/2} I(\phi_e) \cos \phi_e \cdot \cos^2 \phi_e \, d\phi_e}{\int_0^{\pi/2} \mathrm{I}(\phi_e) \cos \phi_e \, d\phi_e}$$

where $I(\phi_e)$ represents the course of the radially integrated peak area with ϕ_e. We have shown[7] that the crystalline orientation factor f_c can be expressed, in the case of yarn containing monoclinic crystals, as $f_c = 3\langle \cos^2 \phi_e \rangle - 2$.

RESULTS AND DISCUSSIONS

Earlier work concerning the influence of spinning conditions on the physical structure of undrawn yarns was carried out by Ishibashi and co-workers[10,11] in 1970 and by Bankar, Spruiell, and White in 1977.[12] As the maximum winding speed mentioned in their papers was only 1000 mpm, there is not much in common with our work in which speeds were used up to 5500 mpm. The x-ray studies in our work have been performed on undrawn yarns after conditioning at 20°C and 60% RH. The radial diffractometer scans of such samples are very poorly resolved, as is illustrated in Figure 5, which shows some equatorial traces (ϕ_e = 0) obtained at various winding speeds. A set of scans, made at different azimuthal angles, is presented in Figure 6. This example originates from an autoclaved sample, merely because this is more suited as an illustration by the better peak separation. As explained before, for each yarn the set of 13 diffractometer scans made at a variety of azimuthal angles is fitted in two successive cycles of calculations with a six-line model. The sixth line takes into account the off-equator intensity at ϕ_e = 15°, due to the 011,210 γ-phase diffraction doublet. In separate runs, the peak position, half-width, and shape parameter were determined as 22.2°, 1.0°, and 1.4, respectively.

Very striking was the finding, after the first cycle of calculations, that not only the various peak intensities but also some other parameters depended on the azimuthal angle ϕ_e. It turned out that also the half-widths of the α 200 and

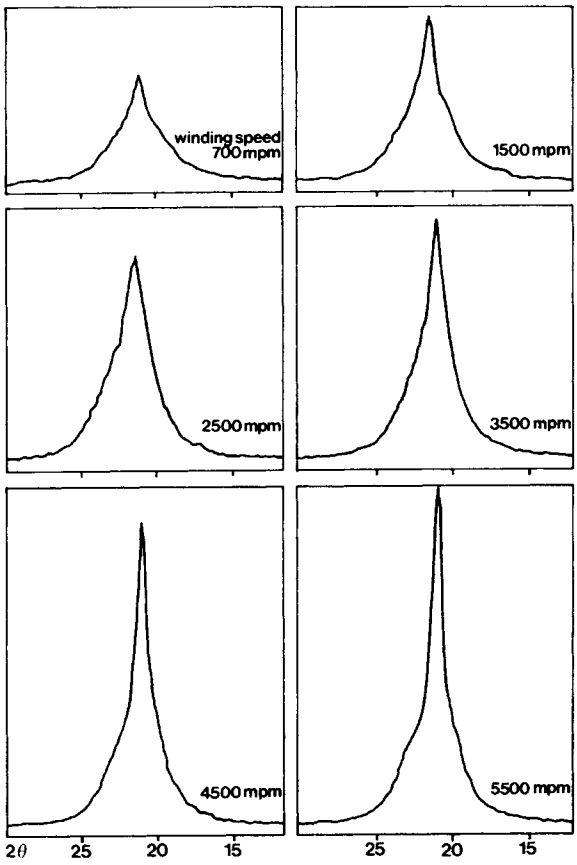

Fig. 5. Equatorial x-ray traces of undrawn nylon 6 yarns, wound at various speeds.

002/202 lines and, in some cases, also the half-widths of the two γ peaks 001 and 200 varied significantly within one set of 13 scans. Therefore, the second run of calculations was carried out with the intensities and these four half-widths as free parameters. It appeared that for significant half-width courses a minimum value was reached at the equator. This means that the thickest crystals are those which are aligned along the fiber axis. As an illustration of this effect in Figure 7, the lateral dimensions of α and γ crystals, as calculated from the 200

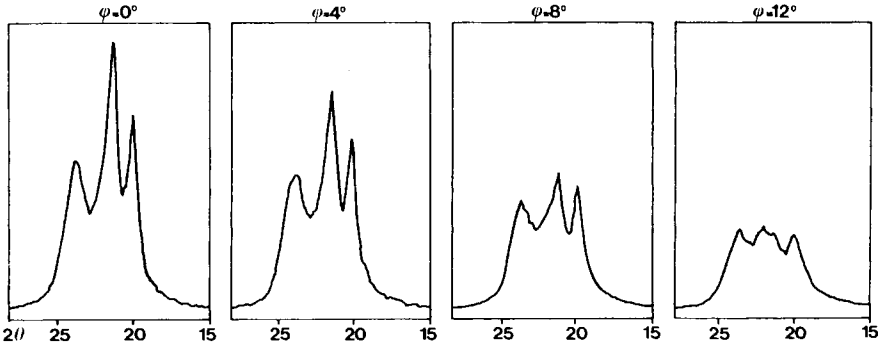

Fig. 6. Radial x-ray traces at various azimuthal angles.

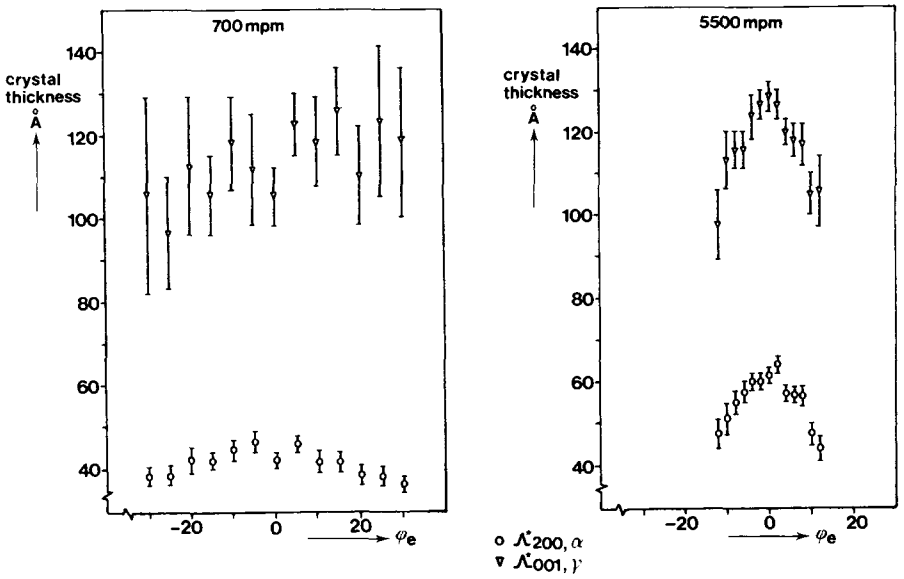

Fig. 7. Crystal thickness as function of azimuthal angle.

α and 001 γ half-widths, are plotted versus ϕ_e. It is clear that the effect for the γ-crystal in the yarn spun at 700 mpm is not significant. For the yarn spun at 5500 mpm, the maximum for both crystal forms is very pronounced. In Figure 8, the crystal thickness of the two crystalline modifications, determined for the equator, is given as a function of the winding speed. Very remarkable is the minimum of the thickness of the γ crystals at about 2500 mpm and the fact that

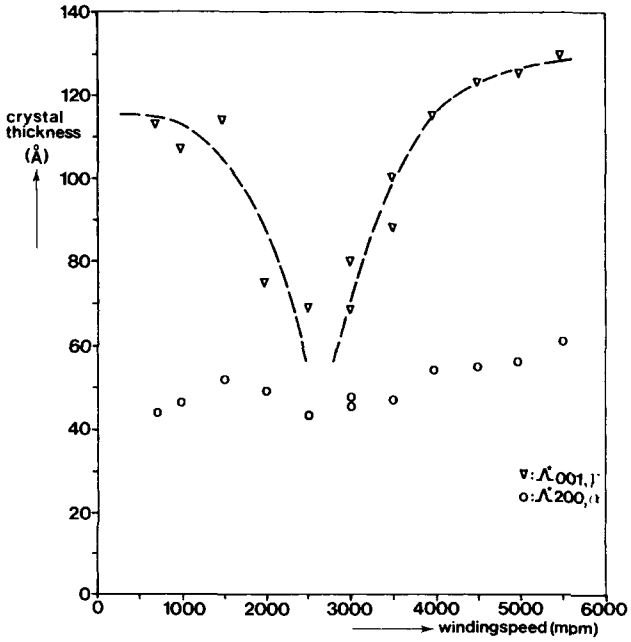

Fig. 8. Crystal thickness as function of winding speed.

the γ crystals have already reached very large lateral dimensions in the as-spun filaments. By using measurements of the meridional 020 diffraction spot, the height of the crystals and the unit cells of the γ-phase crystals could be studied. In the calculation of the height of the unit cell, the Wallner correction was taken into account.[13,14] In Figures 9 and 10, these results are presented. From the course of the radially integrated peak areas of the α 200 and the γ 100 with ϕ_e, illustrated for the two extreme situations in winding speed in Figure 11, the relative γ number and the orientation factors of α and γ were calculated. The results are presented in Figures 12 and 13.

Some of the foregoing results, especially those presented in Figure 8 (γ-crystal thickness) and Figure 13 (orientation factors of α and γ), clearly indicate that two different structure-forming mechanisms for nylon 6 have to be considered. The transition between the two mechanisms is somewhere in between 2000 and 3000 mpm. To ascertain whether also other techniques could contribute to the understanding of the two different branches in the structure-versus-winding speed relation, also DSC and birefringence measurements were carried out. For this purpose, freshly spun, fully dry yarns were investigated by DSC. The results, some of which are presented in Figure 14, make it clear that the crystallization process in these unconditioned yarns did not reach completion during spinning when the yarns were at speeds lower than 3000 mpm. At higher winding speeds, yarns are wound which are already crystalline. So the behavior of dry nylon 6 shows a clear analogy with the behavior described for PET yarns.[15] With respect

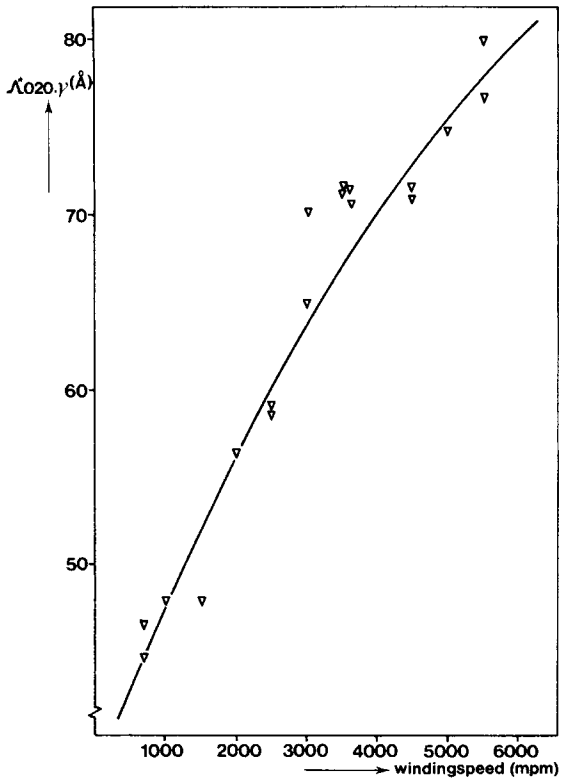

Fig. 9. Height of the γ crystal at various winding speeds.

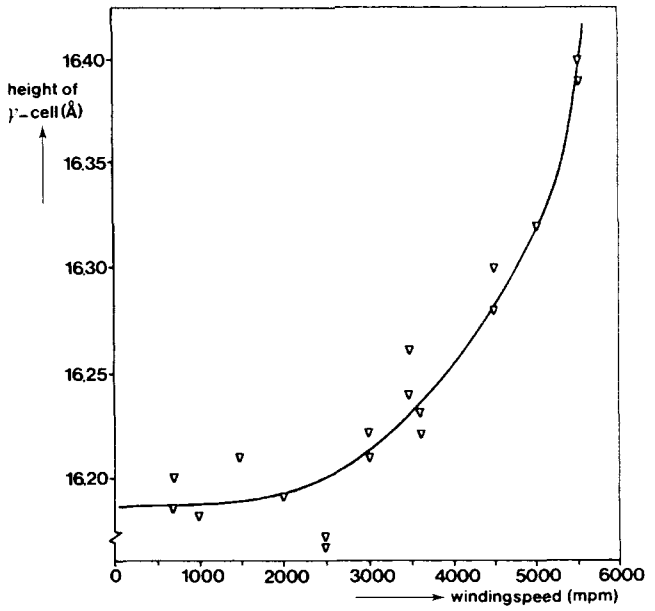

Fig. 10. Height of the γ unit cell vs. winding speed.

to the conditioned yarns, it should be realized that the large difference between nylon 6 and PET is that conditioned nylon 6 is above its glass transition temperature under normal conditions in the winding room. This permits a continuation of the crystallization process under winding room conditions. It follows that the structure present in conditioned yarns spun at lower speeds is mainly due to crystallization after moisture pickup, while the crystals in the yarns wound

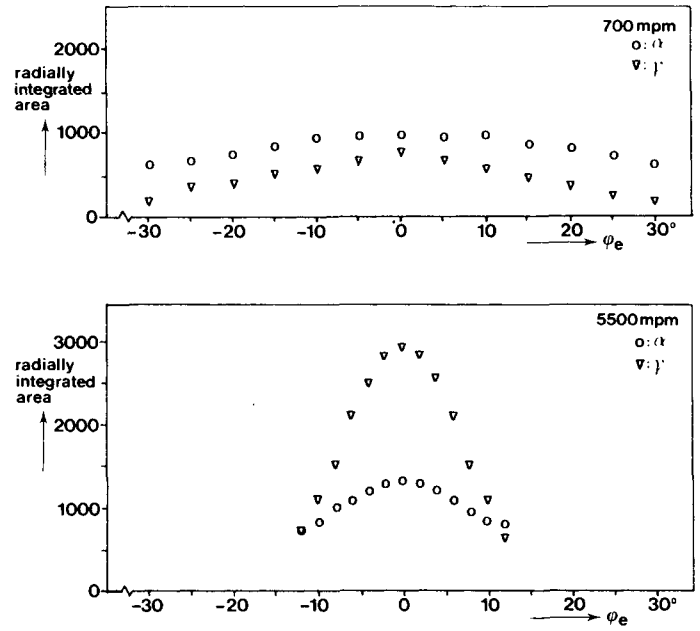

Fig. 11. Integrated peak areas vs. azimuthal angle.

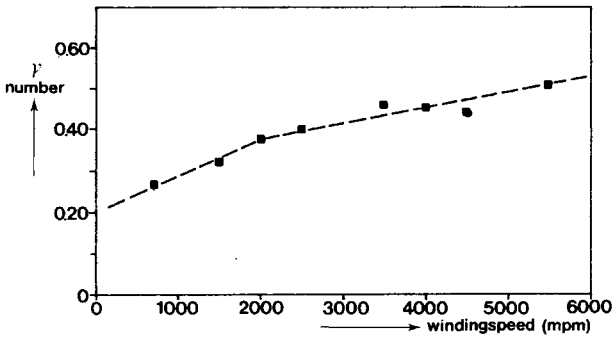

Fig. 12. Influence of winding speed on γ number.

at speeds higher than 3000 mpm are already generated during the spinning process proper. From Figure 12, it follows that the γ-type crystal is favored by an increase in the winding speed. Apparently, the orientation-induced crystallization promotes the γ phase. This is consistent with the very high crystalline orientation factor of that crystal type as illustrated in Figure 13. About the same high value is obtained as in PET yarns wound at very high speeds.[15] In Figure 10, it is shown that the height of the unit cell of the γ crystals formed at speeds exceeding 3000 mpm is a function of the winding speed, which also points to a formation of this crystal type during spinning at high speeds. In the DSC traces (see Fig. 14), at very high winding speeds an additional melting peak occurs on the low-temperature side of the normal melting peak which all samples have in common. Probably the melting point of the γ crystals, after perfectioning in the DSC apparatus, is at most 10 degrees lower than that of the α-type crystals.

While the orientation-induced crystallization phenomenon observed at high winding speeds shows much analogy with the PET case, the crystalline structure of yarns mainly crystallized at a low temperature after moisture pickup still remains to be discussed. From Figure 9 it is clear that the height of the γ crystals is a continuous function of the winding speed. We assume that the height is

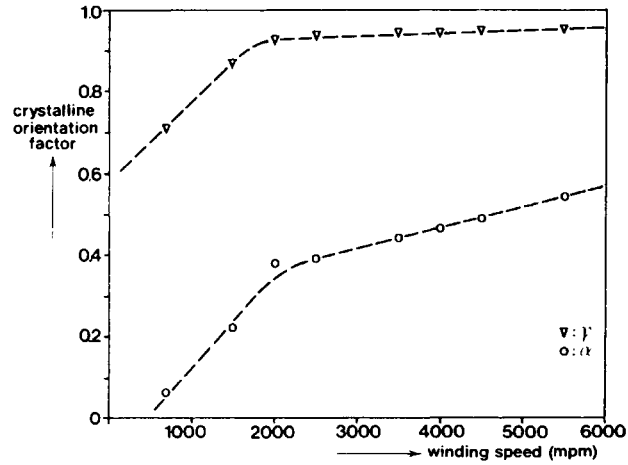

Fig. 13. Effect of winding speed on the orientation of the two crystalline modifications.

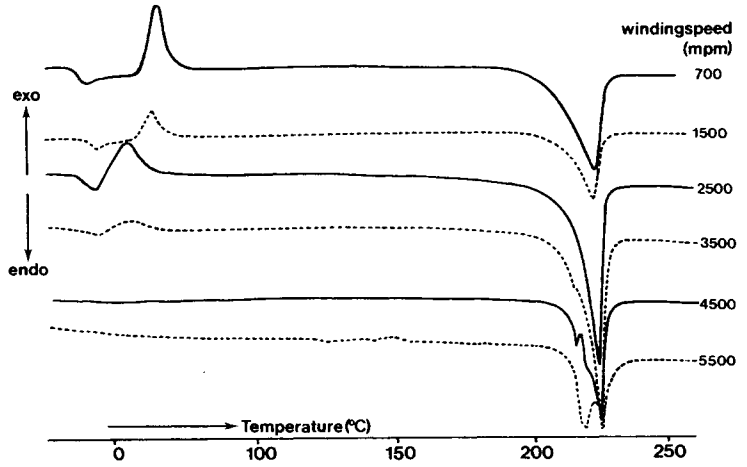

Fig. 14. DSC scans of yarns dry wound at the indicated speeds.

primarily determined by the height of the nuclei spontaneously formed by orientation of the molecules in the spinning process. A high degree of orientation will increase the length over which the molecules can run parallel to each other, higher nuclei being formed in that way. During the crystallization process proper an increase of the thickness of the crystals takes place. So the finding that at low speeds rather thick γ crystals form, as illustrated in Figure 8, seems to suggest that at low winding speeds there is more time available for crystal growth. This could not yet be checked by temperature and velocity measurements in the spinning process because of its complexity. The fact that the α crystals remain very small (see Fig. 8) indicates that the orientation-induced nuclei grow preferentially into γ crystals and that the α crystals grow slowly at low temperatures from nuclei formed by thermal movements of the molecules above the glass transition temperature under the conditions in the winding room. From Figure 13, the orientation of the α crystals appears to be very low in accordance with this view.

In Figure 15, the results of birefringence measurements are presented. The freshly spun, dry wound, and dry measured yarns first show negative birefringences which increase with the winding speed, but the sign changes in the same region of winding speeds where the transition of mechanisms was found by other measuring techniques. At high winding speeds, positive values are found and the differences between dry and conditioned yarns decrease more and more. These results indicate that at high winding speeds the crystallization process is nearly completed before moisture pickup. By contrast, the large change in birefringence taking place during conditioning of the as-spun yarns wound at low speeds points to appreciable structural changes of these yarns during wetting. Birefringence measurements therefore support the view that two different crystallization mechanisms are involved, one predominating at winding speeds above 2500 mpm and the other in the region of lower winding speeds.

The foregoing rather complex picture of what is going on during winding of undrawn nylon 6 filaments can be summarized as follows: An increase of the winding speed favors the formation of the γ-phase crystals. These seem to form from orientation-induced nuclei, giving rise to well-oriented γ-phase crystals.

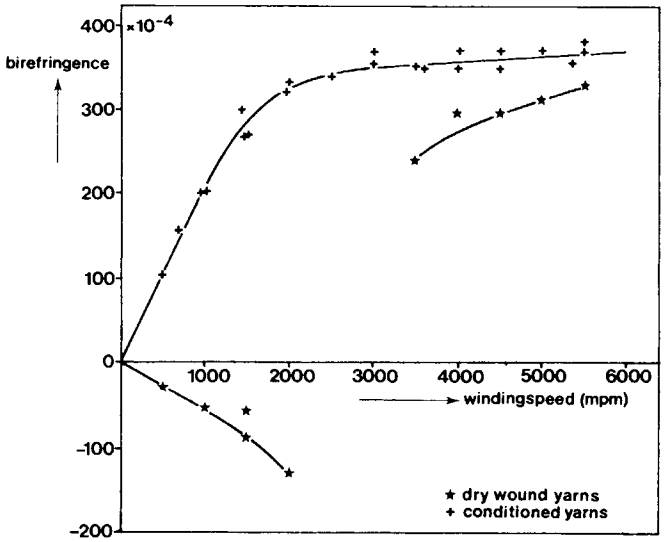

Fig. 15. Effect of winding speed on conditioned and dry wound as-spun yarns.

At high winding speeds, the crystallization process approaches completion during spinning, resulting in a structure consisting of a mixture of large, well-oriented γ crystals and small α crystals with lower orientation. At low winding speeds, this crystallization mainly takes place immediately after wetting, possibly on the bobbin. In that process, small, nearly unoriented α crystals form apart from a small amount of γ crystals which are moderately oriented and small in the direction of the molecules. In lateral direction, the γ crystals reach a minimum value between 2000 and 3000 mpm, a transition region which is also indicated by DSC, birefringence, and additional x-ray information on the height of the γ unit cell and the two crystalline orientation factors.

Yarns Heat-Treated at Various Temperatures and Drawn at Various Ratios

To investigate the effect of temperature and tension on the crystalline structure of nylon 6, three winding speeds were selected for further experiments. These speeds were 1460, 3630, and 5325 mpm. The undrawn yarns were heat treated *in vacuo* in an oven at 150, 180, and 210°C. At the same temperatures also drawing experiments were performed. This process used an electrically heated hotplate, 34 cm in length, three wraps, and a speed of 400 mpm. Structural investigations were carried out on yarns drawn at the lowest possible draw ratio (criterion: no undrawn parts) and the highest possible draw ratio (criterion: breakage). In Figure 16, the "γ number" is shown in relation to heat-treatment temperature and draw ratio. Lines have been drawn for the tensionless heated samples. A comparison of these lines for the three winding speeds shows that for all three cases the same shape is found with a shift toward higher temperatures for higher winding speeds. The decrease on the high-temperature side is thought to be caused by melting of the γ crystals, this process depending on the crystal size. So the short γ crystals formed in the yarn spun at 1460 mpm disappear above 180°C, those present in the yarn spun at 3630 mpm disappear above 190°C,

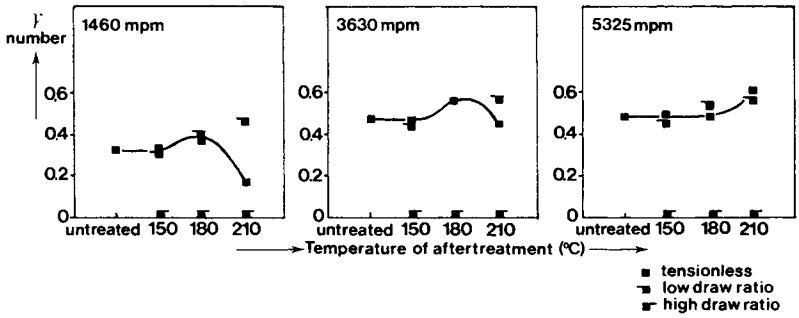

Fig. 16. Effect of temperature and drawing on the content of γ crystals.

while the long, large crystals in the yarn spun at 5500 mpm are stable up to at least 210°C, the highest temperature used in these experiments.

The fact that there is a region where the "γ number" increases suggests that at temperatures a little below the onset of the melting of the γ crystals, the very small α crystals are unstable with respect to the large γ crystals. When heating is combined with a low draw ratio, about the same results with respect to the "γ number" are obtained, except in cases where melting occurs in the tensionless state. The application of some tension causes an increase of the melting temperature because it reduces the entropy gain during melting. This effect can clearly be observed in Figure 16 for 1460 and 3630 mpm at 210°C, where apparently no melting of the γ-phase crystals occurs under tension. If high draw ratios are applied, the "γ number" drops to negligible values. This effect is in accordance with findings of other investigators.[16] The application of high draw ratios apparently causes such tensions on the chains in the γ crystal that the slightly twisted molecules in the shorter γ unit cell are forced to assume the extended zigzag configuration characteristic of the α-crystal form. In Figure 17, the crystalline orientation factors for both crystalline modifications are given. As can be seen, the γ modification is very well oriented in all cases, and there are

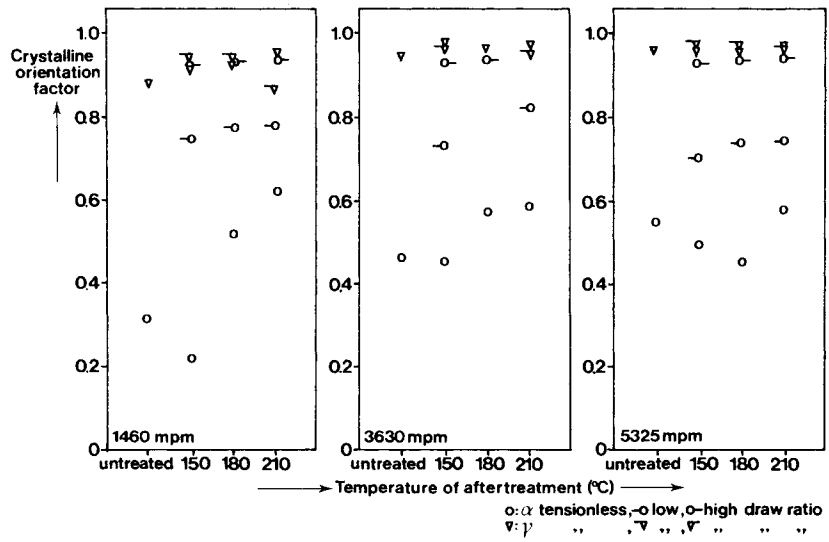

Fig. 17. Effect of temperature and drawing on the orientation of the two crystal forms.

no significant differences between yarns heated tensionless and those heated at a low draw ratio.

On the orientation of the α modification, however, drawing has a pronounced effect. At the highest draw ratio, the α crystals reach eventually the same high level of orientation as the original γ crystals. The increase of the orientation factor of the α crystals, as found in the case of the two lower winding speeds in heating tensionless at increasing temperature, may be related to the direction dependence of the crystal size as already presented in Figure 7. The less oriented crystals are smaller and consequently less stable. So if partial melting takes place, primarily the least-oriented crystals will vanish, resulting in a higher crystalline orientation factor after such a heat treatment. That this effect is not found for the yarn spun at 5325 mpm may be due to the larger crystals in that case.

The effect of drawing has in the foregoing only been illustrated with results obtained from yarns drawn at the "lowest" and the "highest" possible draw ratio. In order to gain some more insight into the course of the "γ number" and the two crystalline orientation factors with the draw ratio, we investigated a series of six draw ratios applied at 180°C to the yarn wound at 5325 mpm. In Figure 18, the γ number is presented; both crystalline orientation factors are presented in Figure 19. From the course of the γ number it follows that the breakdown of the γ crystals is not an abrupt but a rather gradual process. Concerning the crystalline orientation factors, the most remarkable result is the decrease of the orientation factor of the γ crystals at high draw ratios. The reason is that drawing is most effective with respect to well-oriented crystals. These crystals are selectively forced to convert into the α modification, and consequently the average orientation of the remaining γ crystals decreases.

With respect to the crystal dimensions, the general trend is that the dimensions Λ^*_{020} (γ, height), Λ^*_{011} (γ, thickness) and Λ^*_{200} (α, thickness) increase with the temperature of the after-treatment. This increase scarcely depends on the draw ratio. The only remarkable result is that an extra increase of the Λ^*_{200} (α, thickness) is found for cases where the γ crystals have disappeared by melting. Accordingly, for yarns, wound at 1460 and 3630 mpm and heated tensionless at 210°C, Λ^*_{200} values of 148 and 121 Å, respectively, were found. Summarizing the

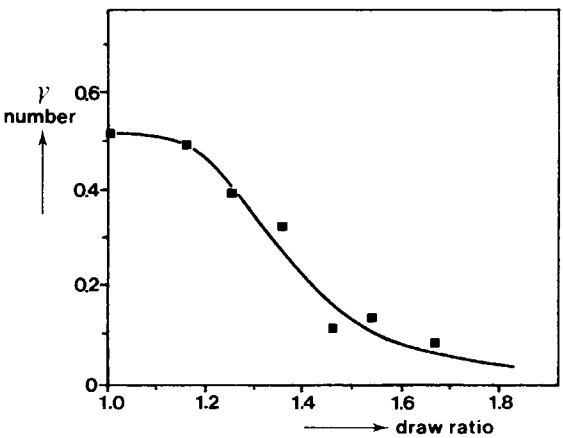

Fig. 18. Gamma number as function of draw ratio.

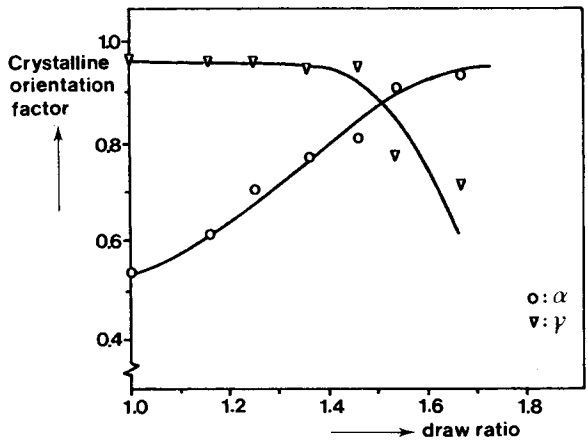

Fig. 19. Influence of drawing on the two crystalline orientation factors.

most important results, it can be stated that drawing causes a gradual transition from γ- to α-type crystals. The high orientation of the γ crystals is unaffected by those aftertreatments which do not overcharge the mechanical stability of the crystals. The orientation of the α crystals increases during drawing and reaches the level of the γ orientation at very high draw ratios at which the γ modification disappears. Small γ crystals, especially with low Λ^*_{020} values, as found in yarns spun at low speeds, can vanish by partial melting, in which case extremely thick α crystals form with a much better orientation than the original α crystals.

Aftertreatments with Saturated Steam

From a practical point of view, autoclaving with saturated steam is important for the heat setting of yarns. Therefore, the three yarns wound at 1460, 3630, and 5325 mpm were autoclaved each at 110, 120, and 130°C in the fully tensionless state. In Figure 20, the equatorial x-ray diffractometer scans are shown. From these pictures, it is clear that autoclaving causes a considerable decrease of the amount of γ-type crystals. Also for these yarns, complete sets of ϕ_e scans were made to determine γ numbers and crystalline orientation factors. In Figure 21, the course of the γ number as a function of the autoclaving temperature is presented. It is quite obvious that the γ modification is not resistant to these severe heat treatments. Only the large crystals in the yarn wound at 5325 mpm are stable with respect to the treatment at 110°C. The course of the crystalline orientation functions (see Fig. 22) shows an appreciable increase of the orientation for the α-type crystals. As it was found that the decrease of the amount of γ crystals was accompanied by an increase of the amount of α crystals, it has to be assumed that the γ crystals which vanished recrystallize in the form of α crystals. Since a part of the better-oriented molecules thus recrystallizes in α-type crystals, this explains the increase in crystalline orientation factor of the α modification. The newly formed, strongly predominating α phase appears to consist of very thick crystals. Being roughly independent of the winding speed, the values obtained are about 110 Å at 110°C, 125 Å at 120°C, and 145 Å at 130°C. When the structural data of the autoclaved yarns are compared with

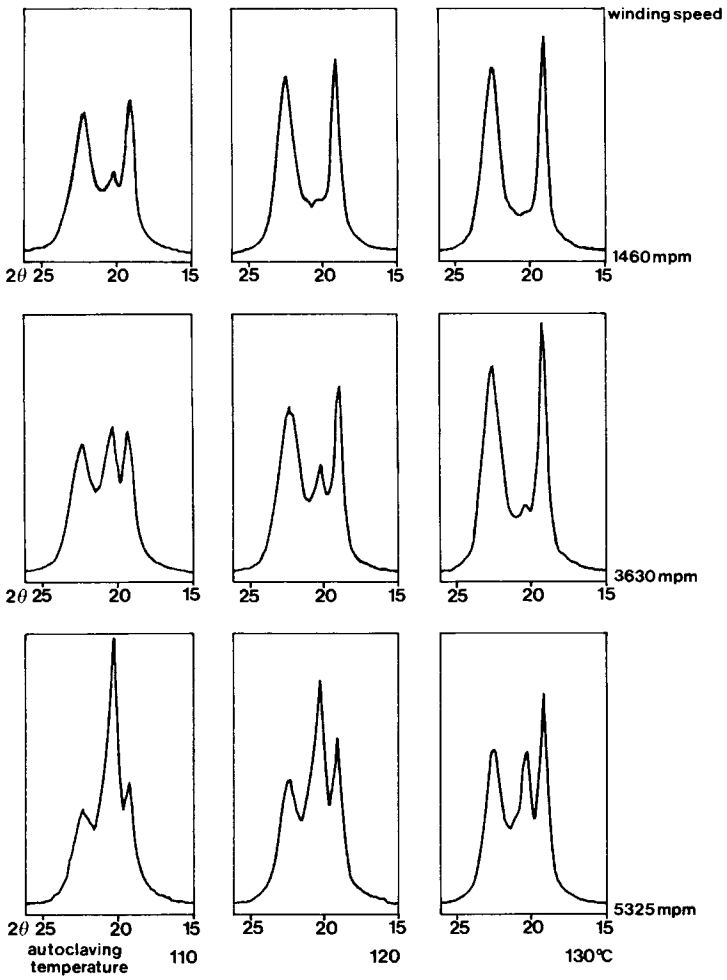

Fig. 20. Equatorial x-ray diffraction patterns of undrawn yarns wound at different speeds and autoclaved at various temperatures.

those obtained by a heat treatment *in vacuo*, it appears that Figure 21 can be considered as an extension of Figure 16 to higher temperatures. The same kind of relation holds for Figures 17 and 22. This suggests that the autoclaving procedure, i.e., working with saturated steam, is directly comparable with heating

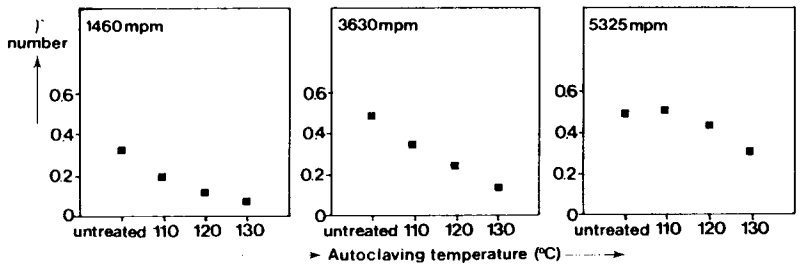

Fig. 21. Effect of autoclaving temperature on amount of γ-type crystals.

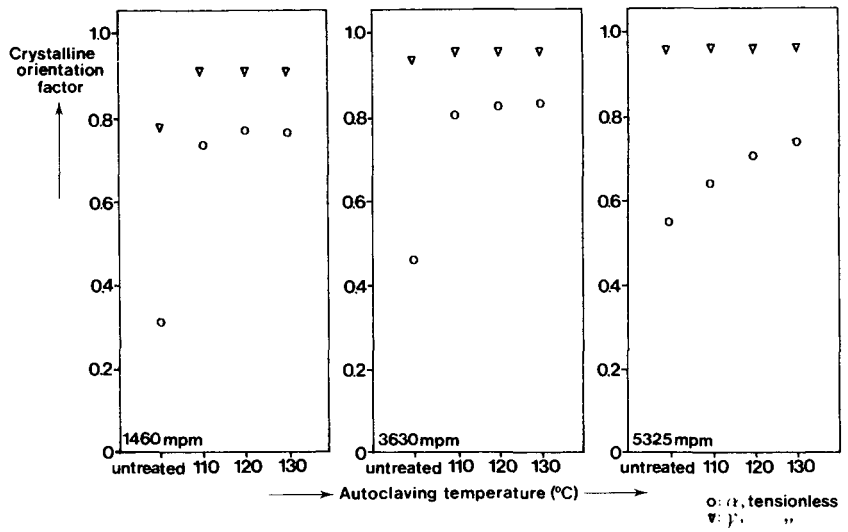

Fig. 22. Orientation of both crystalline modifications as a function of autoclaving conditions.

in vacuo but at extremely high temperatures. In other words, the moisture favors the mobility of the molecules, by loosening the hydrogen bonds, to such a large extent that a given temperature in saturated steam corresponds with a much higher temperature in the dry state.

The effect of autoclaving can be summarized as a partial conversion of γ-type crystals to the α type, an increase of the α orientation, and a substantial coarsening of the α structure, brought about by the somewhat lower heat stability of the γ-type crystals. This again supports the idea that the α modification is the more stable crystal form from the energy point of view. The fact that γ crystals can form during spinning shows that for orientation-induced crystallization the kinetics are in favor of this crystal type.

The authors express their thanks to the following who were directly involved in this work connected with many different disciplines: A. Compagnie for autoclaving the yarns; L. J. Lucas for his computer work and birefringence measurements; M. Mannee for his computer work; M. J. G. van de Mortel for his spinning and drawing experiments; M. G. Northholt for his calculations of the Wallner corrections; A. Vakkers for performing the x-ray measurements; J. M. Woestenenk for birefringence work and stimulating interest; and J. de Wit for his DSC measurements.

References

1. D. R. Holmes, C. W. Bunn, and D. J. Smith, *J. Polym. Sci.*, **17**, 159 (1955).
2. H. Arimoto, *J. Polym. Sci. Part A*, **2**, 2283 (1964).
3. D. C. Vogelsong, *J. Polym. Sci. Part A*, **1**, 1055 (1963).
4. E. M. Bradbury, L. Brown, A. Elliott, and D. D. Parry, *Polymer*, **6**, 465 (1964).
5. K. H. Illers, H. Haberkorn, and P. Simák, *Makromol. Chem.*, **158**, 285 (1972).
6. R. F. Stepaniak, A. Garton, D. J. Carlsson, and D. M. Wiles, *J. Appl. Polym. Sci.*, **17**, 987 (1979).
7. H. M. Heuvel and R. Huisman, to be published.
8. R. F. Stepaniak, A. Garton, D. J. Carlsson, and D. M. Wiles, *J. Appl. Polym. Sci.*, **23**, 1747 (1979).
9. L. E. Alexander, *X-Ray Diffraction Methods in Polymer Science*, Wiley–Interscience, New York, 1969, pp. 241–279.
10. T. Ishibashi, K. Aoki, and T. Ishii, *J. Appl. Polym. Sci.*, **14**, 1597 (1970).
11. T. Ishibashi and T. Ishii, *J. Appl. Polym. Sci.*, **20**, 335 (1976).

12. V. G. Bankar, J. E. Spruiell, and J. L. White, *J. Appl. Polym. Sci.*, **21,** 2341 (1977).
13. L. G. Wallner, *Monatsh. Chem.*, **79,** 279 (1948).
14. M. G. Northolt and H. A. Stuut, *J. Polym. Sci.*, **16,** 939 (1978).
15. H. M. Heuvel and R. Huisman, *J. Appl. Polym. Sci.*, **22,** 2229 (1978).
16. K. Miyasaka and K. Makishima, *J. Polym. Sci., Part A1,* **5,** 3017 (1967).

Received August 13, 1980
Accepted August 26, 1980